

Dynamics of an axisymmetric body spinning on a horizontal surface. II. Self-induced jumping

Y Shimomura, M Branicki and H.K Moffatt

Proc. R. Soc. A 2005 **461**, doi: 10.1098/rspa.2004.1429, published 8 June 2005

References

This article cites 7 articles, 1 of which can be accessed free
<http://rspa.royalsocietypublishing.org/content/461/2058/1753.full.html#ref-list-1>

Article cited in:
<http://rspa.royalsocietypublishing.org/content/461/2058/1753.full.html#related-urls>

Email alerting service

Receive free email alerts when new articles cite this article - sign up in the box at the top right-hand corner of the article or click [here](#)

Dynamics of an axisymmetric body spinning on a horizontal surface. II. Self-induced jumping

BY Y. SHIMOMURA¹, M. BRANICKI² AND H. K. MOFFATT²

¹*Department of Physics, Keio University, Hiyoshi, Yokohama 223-8521, Japan*
(yutaka@phys-h.keio.ac.jp)

²*Department of Applied Mathematics and Theoretical Physics,
Wilberforce Road, Cambridge CB3 0WA, UK*
(mb388@damtp.cam.ac.uk; hkm2@damtp.cam.ac.uk)

Following part I of this series, the general spinning motion of an axisymmetric rigid body on a horizontal table is further analysed, allowing for slip and friction at the point of contact. Attention is focused on the case of spheroids whose density distribution is such that the centre-of-mass and centre-of-volume coincide. The governing dynamical system is treated by a multiple-scale technique in order to resolve the two time-scales intrinsic to the dynamics. An approximate solution for the high-frequency component of the motion reveals that the normal reaction can oscillate with growing amplitude, and in some circumstances will fall to zero, leading to temporary loss of contact between the spheroid and the table. The exact solution for the free motion that ensues after this ‘jumping’ is analysed, and the time-dependence of the gap between the spheroid and the table is obtained up to the time when contact with the table is re-established. The analytical results agree well with numerical simulations of the exact equations, both up to and after loss of contact.

Keywords: rigid body dynamics; dynamical systems; self-induced jumping; spinning spheroid; gyroscopic approximation; Jellett constant

1. Introduction

In a brief communication, hereafter referred to as MS’02, [Moffatt & Shimomura \(2002\)](#) discussed the familiar phenomenon of the rise to the vertical of a hard-boiled egg set in rapid spinning motion on a table. The governing equations were simplified under the dual assumptions that the friction is weak and the spin is large (so that the Coriolis force is dominant). Under this ‘gyroscopic’ approximation, a first-order differential equation for the inclination of the axis of symmetry was obtained, which, for the case of a prolate spheroid, did indeed describe the rise of the axis to the vertical. This rise was associated with the effect of the weak friction (measured by a dimensionless parameter $\mu \ll 1$) at the point of contact and occurred on a ‘slow’ time-scale $O(\mu^{-1})$, irrespective of the nature of the frictional force (‘dry’ Coulomb friction or ‘wet’ viscous friction). However, this rising motion is accompanied by fluctuations occurring on a ‘fast’

$O(1)$ time-scale. A linear stability analysis by Moffatt *et al.* (2004; hereafter referred to as part I) showed the existence of modes oscillating on the fast time-scale. These slow and fast time-scales intrinsic to the dynamics are well separated when $\mu \ll 1$.

In the above papers, the analysis and computations were restricted to circumstances in which the normal reaction R remains positive and the spheroid remains in contact with the table throughout the motion. However, in some regions of parameter space, the growth of the fluctuations allows R to decrease to zero. In the present paper, we analyse these fluctuations which depend on the two time-scales, with a view to determining their effect on the dynamics. First, the two time-scales are formally introduced and the mean part of the motion (which is identical to the solution found by MS'02 under the gyroscopic approximation) is defined by filtering out the fast oscillations. The fluctuating part is then analysed up to $O(\mu)$ by the WKB method, in order to derive the time-dependence of R . Numerical simulation of the governing sixth-order nonlinear dynamical system is carried out in order to test the validity of the analytical results. The location of the surface $R=0$ in the 'gyroscopic subspace' is derived analytically and confirmed by the simulation.

When a trajectory crosses this surface, the dynamical regime changes, the spheroid being then subject only to the influence of gravity. We analyse this 'free motion' (for which an exact analytical solution is available—see, for example, Marsden & Ratiu 1999) in §4, and we determine the time-dependence of the gap $\Delta(t)$ between the spheroid and the table during the brief period of free flight before contact is re-established. Again, the results are in good accord with numerical simulation.

The rising motion described above is associated with a non-oscillatory mode of instability whose growth rate is $O(\mu)$, and which therefore exists only by virtue of the dissipative frictional force at the point of contact between the spheroid and the table. Instabilities of this kind have been treated from a geometrical point of view by Bloch *et al.* (1994), who describe them as 'dissipation-induced instabilities'; the approach, which is complementary to ours, has been recently developed by Bou-Rabee *et al.* (2004, 2005) and applied to the problem of the spinning prolate spheroid. These authors have determined conditions under which a heteroclinic orbit connects an unstable state (with axis horizontal) with a stable state (with axis vertical). We shall find that the growth of oscillatory modes in the neighbourhood of such heteroclinic orbits can trigger loss of contact between the spheroid and table, implying a fundamental modification of the governing dynamical system.

The behaviour after the first period of free flight depends on the physical properties of both solids, which determine the precise nature of the subsequent 'bouncing' process (not analysed in this paper). We may, however, conjecture that the averaged behaviour (over many successive impacts) will be simply to give an 'effective' Coulomb friction parameter μ_e somewhat less than the value of μ that pertains during periods of continuous contact.

2. Geometry and dynamical equations

Let us first recapitulate the essential notations and equations for the problem, as presented in part I. We consider the dynamics of a rigid axisymmetric body with

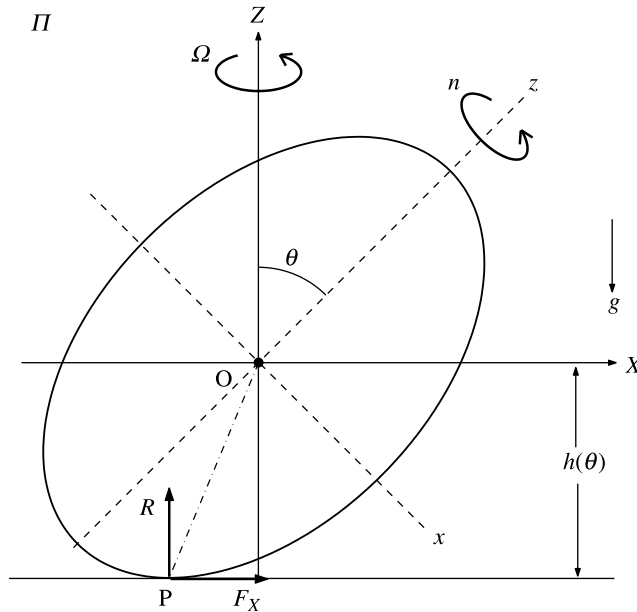


Figure 1. Sketch of the system defining the notation.

centre-of-volume O and surface S which moves on a horizontal table, making sliding and/or rolling contact at a point P (figure 1). We restrict attention in this paper to bodies that are ‘flip-symmetric’, i.e. symmetric about the plane Oxy perpendicular to the axis of symmetry Oz . (The effects of flip symmetry breaking will be deferred to a subsequent paper, part III in this series.) With Ox in the plane defined by Oz and the vertical OZ , we may use $Oxyz$ as a rotating frame of reference. Alternatively, we may use $OXYZ$, where OX is horizontal and OY coincides with Oy .

Let M be the mass of the body and b its radius of cross-section in the plane Oxy . We use dimensionless variables based on $(M, b, (b/g)^{1/2})$ as units of mass, length and time. We denote the dimensionless principal moments of inertia at O by (A, A, C) .

Six variables are needed to define the state of motion of the body: $(U, V, \Omega, A, \theta, n)$, where (U, V) are the X - and Y -components of velocity of O , Ω is the rate of precession of Oz about OZ , θ is the angle between Oz and OZ , $A = \dot{\theta}$, and n is the spin (i.e. the component of angular velocity about Oz). The dynamical evolution is described by trajectories in the six-dimensional phase-space of these variables.

Let $h(\theta)$ be the height of O above the table. Then the coordinates of P (part I, eqn (2.7)) are given by

$$\mathbf{X}_P = (X_P, Y_P, Z_P) = \left(\frac{dh}{d\theta}, 0, -h \right), \quad (2.1)$$

or equivalently by

$$x_P = -h^2 \frac{d}{d\theta} \left(\frac{\cos \theta}{h} \right), \quad z_P = -h^2 \frac{d}{d\theta} \left(\frac{\sin \theta}{h} \right). \quad (2.2)$$

The velocity of the point P (of the body) is

$$\mathbf{U}_P = U_P \mathbf{I} + V_P \mathbf{j} + W_P \mathbf{K}, \quad (2.3)$$

where

$$U_P = U - h\Lambda, \quad (2.4a)$$

$$V_P = V - h^2(n - \Omega \cos \theta) \frac{d}{d\theta} \left(\frac{\cos \theta}{h} \right) + \Omega \frac{dh}{d\theta}, \quad (2.4b)$$

$$W_P = W - \Lambda \frac{dh}{d\theta}; \quad (2.4c)$$

W is the vertical component of velocity of O, and \mathbf{I} , $\mathbf{J}(=\mathbf{j})$, \mathbf{K} are unit vectors in the directions OX, OY ($=Oy$) and OZ. For so long as the body remains in contact with the table, we have $W_P = 0$, and so

$$W = \Lambda \frac{dh}{d\theta}. \quad (2.5)$$

Let R be the normal reaction and $\mathbf{F} = F_X \mathbf{I} + F_y \mathbf{j}$ the horizontal frictional force at P. Unless otherwise stated, we shall use the Coulomb friction model for which

$$\mathbf{F} = F_X \mathbf{I} + F_y \mathbf{j} = -\mu R \frac{\mathbf{U}_P}{|\mathbf{U}_P|}, \quad (2.6)$$

where μ is a positive constant, assumed small. As derived in part I, the governing evolution equations are

$$\dot{U} = \Omega V + F_X, \quad (2.7a)$$

$$\dot{V} = -\Omega U + F_y, \quad (2.7b)$$

$$\dot{\Omega} = \frac{1}{A \sin \theta} \left[Cn\Lambda - 2A\Omega\Lambda \cos \theta - h^2 F_y \frac{d}{d\theta} \left(\frac{\sin \theta}{h} \right) \right], \quad (2.7c)$$

$$\dot{\Lambda} = \frac{1}{A} \left[\Omega \sin \theta (A\Omega \cos \theta - Cn) - R \frac{dh}{d\theta} - hF_X \right], \quad (2.7d)$$

$$\dot{\theta} = \Lambda, \quad (2.7e)$$

$$\dot{n} = -\frac{h^2 F_y}{C} \frac{d}{d\theta} \left(\frac{\cos \theta}{h} \right). \quad (2.7f)$$

For as long as the body remains in contact with the table, the normal reaction R is given by

$$R = 1 + \dot{W} = 1 + \frac{d}{dt} \left(\Lambda \frac{dh}{d\theta} \right), \quad (2.8)$$

and satisfies the constraint

$$R \geq 0. \quad (2.9)$$

For the particular case of a flip-symmetric spheroid of aspect ratio a (prolate or oblate accordingly as $a >$ or < 1), $h(\theta)$ is given by

$$h(\theta) = (a^2 \cos^2 \theta + \sin^2 \theta)^{1/2}, \quad \frac{dh}{d\theta} = \frac{(1 - a^2) \cos \theta \sin \theta}{h}. \quad (2.10)$$

Attention will be focused on this case in this paper. These formulae are used in evaluating the integrals in §3*d*.

3. Multiple-scale analysis

We now use the multiple-scale method (e.g. [Hinch 1992](#); [Holmes 1995](#)) to analyse the above system. The approach is similar to that developed by [Yoshizawa \(1984, 1998\)](#) in a statistical treatment of inhomogeneous turbulence. Only flip-symmetric bodies are considered in this paper.

(a) Introduction of two scales

First, guided by the form of (2.7*d*), we replace n with a new variable Ψ defined by

$$\Psi = A^{-1}(A\Omega \cos \theta - Cn) \sin \theta. \quad (3.1)$$

In the $Oxyz$ frame, defined by the rotation formulae

$$x = X \cos \theta - Z \sin \theta, \quad y = Y, \quad z = X \sin \theta + Z \cos \theta, \quad (3.2)$$

(2.7*c-f*) can be written in the form

$$\frac{d}{dt}(\Omega - \Psi \cot \theta) = \frac{h_\theta F_y}{A}, \quad (3.3a)$$

$$\frac{d\Psi}{dt} + \Omega \frac{d\theta}{dt} = -\frac{hF_y}{A}, \quad (3.3b)$$

$$\frac{d^2\theta}{dt^2} - \Omega\Psi = -\frac{1}{A}(h_\theta R + hF_x), \quad (3.3c)$$

with R given by (2.8) and $h_\theta = dh/d\theta$. Equations (2.7*a,b*) are only weakly coupled with (3.3) when $\mu \ll 1$ (for $\mu = 0$, they are decoupled); we shall find below that they have no effect on the analysis up to $O(\mu)$, provided that the initial horizontal velocity of the centre-of-mass is not greater than $O(\mu)$.

As discussed and motivated in §1, we now distinguish slow and fast time variables T and τ defined by

$$T = \mu t, \quad \tau = t \quad (\mu \ll 1), \quad (3.4)$$

and assume that any variable f depends on both T and τ : $f = f(T, \tau)$. Note that then

$$\frac{df}{dt} = \frac{\partial f}{\partial \tau} + \mu \frac{\partial f}{\partial T}. \quad (3.5)$$

The mean \bar{f} is defined as the fast-time average

$$\bar{f}(T) = \frac{1}{2\tau_\infty} \int_{-\tau_\infty}^{\tau_\infty} f(T, \tau') d\tau', \quad (3.6)$$

where τ_∞ is large enough to filter out the fast motion and yet small enough to resolve the slow motion. The fluctuating part of f is then given by

$$f'(T, \tau) = f - \bar{f}(T), \quad \bar{f}' = 0. \quad (3.7)$$

(b) *Equations for mean variables*

We now assume that the fluctuations in θ , Ω and Ψ are weak, i.e. that

$$|\theta'| \ll 1, \quad |\Omega'| \ll 1, \quad |\Psi'| \ll 1, \quad (3.8)$$

and we linearize in the fluctuations. Then, in particular, defining $\hat{V}_P = \bar{V}_P / |\bar{V}_P|$, we have

$$\bar{U}_P = O(\mu), \quad U'_P = -h \frac{\partial \theta'}{\partial \tau} + O(\mu), \quad (3.9)$$

$$\bar{V}_P = \frac{A - a^2 C}{Ch} \bar{\Omega} \sin \bar{\theta} \cos \bar{\theta} + O(\mu), \quad (3.10)$$

$$\bar{F}_X = O(\mu^2), \quad F'_X = \frac{\mu h}{|\bar{V}_P|} \frac{\partial \theta'}{\partial \tau} + O(\mu^2), \quad (3.11)$$

$$\bar{F}_y = -\mu \hat{V}_P + O(\mu^2), \quad F'_y = -\mu R' \hat{V}_P + O(\mu^2), \quad (3.12)$$

$$\bar{R} = 1 + O(\mu^2), \quad R' = h_\theta \frac{\partial^2 \theta'}{\partial \tau^2} + 2\mu \left(h_\theta \frac{\partial^2 \theta'}{\partial T \partial \tau} + h_{\theta\theta} \frac{d\bar{\theta}}{dT} \frac{\partial \theta'}{\partial \tau} \right) + O(\mu^2), \quad (3.13)$$

where from now on h , h_θ , $h_{\theta\theta}$, ... represent h , $dh/d\theta$, $d^2h/d\theta^2$, ... evaluated at $\theta = \bar{\theta}$. Here, several points may be noted by way of physical interpretation: first, $\bar{R} \approx 1$ represents the approximate balance between the weight of the spheroid and the normal reaction at P; second, the first contribution to R' may become $O(1)$ if $\bar{\Omega}$ is large enough (see equations (3.29) and (3.30) below). Finally, \bar{F}_y is first-order in μ , whereas \bar{F}_X is second-order; this was already recognized within the gyroscopic approximation by MS'02; it is indeed the component \bar{F}_y which is responsible for the rise of the spheroid.

It should perhaps be emphasized here that in the above expressions and all similar formulae, the parameter μ is small, but non-zero. If μ is zero, then the scale separation, on which the treatment is based, is no longer available.

The mean parts of equations (3.3) linearized in the fluctuations give

$$\frac{d}{dT}(\bar{\Omega} - \bar{\Psi} \cot \bar{\theta}) = \frac{h_\theta \bar{F}_y}{\mu A}, \quad (3.14a)$$

$$\frac{d\bar{\Psi}}{dT} + \bar{\Omega} \frac{d\bar{\theta}}{dT} = -\frac{h \bar{F}_y}{\mu A}, \quad (3.14b)$$

$$\mu^2 \frac{d^2 \bar{\theta}}{dT^2} - \bar{\Omega} \bar{\Psi} = -\frac{1}{A}(h_\theta + h \bar{F}_x). \quad (3.14c)$$

If we assume the gyroscopic condition (MS'02) in the form

$$\bar{\Omega} \gg 1, \quad (3.15)$$

then, from (3.14c), $\bar{\Psi} \approx h_\theta / A \bar{\Omega}$ is small and at leading order (in both μ and $\bar{\Omega}^{-1}$) equations (3.14a,b) approximate to

$$\frac{d\bar{\Omega}}{dT} = -\frac{h_\theta \hat{V}_P}{A}, \quad (3.16a)$$

$$\bar{\Omega} \frac{d\bar{\theta}}{dT} = \frac{h \hat{V}_P}{A}. \quad (3.16b)$$

From these equations, the Jellett constant,

$$J = A \bar{\Omega} h, \quad (3.17)$$

is easily obtained, and the gyroscopic solution for the nonlinear system (3.16) is then found as in MS'02. For a uniform spheroid under Coulomb friction, this gyroscopic solution for $\bar{\theta}$ with initial value $\bar{\theta}_0 \in (0, \pi/2)$ is

$$\tan \bar{\theta} = -a \tan q(T - T_0), \quad (3.18)$$

where q and T_0 are given by

$$q = \frac{a(a-1)}{J|a-1|}, \quad a \tan qT_0 = \tan \bar{\theta}_0. \quad (3.19)$$

This solution describes a monotonic increase of h , i.e. a rising motion of the centre-of-mass, as observed in prolate spinning eggs or oblate stones as used in the game of Go. Here, we should note that the mean parts $\bar{\theta}$, $\bar{\Omega}$ and $\bar{\Psi}$ in the present formulation correspond precisely to the gyroscopic solution obtained in MS'02.

(c) Analysis of the fluctuations

By subtracting the mean equations from the exact equations (3.3), the linearized equations for the fluctuations are found in the form:

$$\left(\frac{\partial}{\partial \tau} + \mu \frac{\partial}{\partial T} \right) \left(\Omega' - \Psi' \cot \bar{\theta} + \frac{\bar{\Psi}}{\sin^2 \bar{\theta}} \theta' \right) = \frac{1}{A} (h_{\theta\theta} \bar{F}_y \theta' + h_\theta F_y'), \quad (3.20)$$

$$\frac{\partial \Psi'}{\partial \tau} + \bar{\Omega} \frac{\partial \theta'}{\partial \tau} = -\frac{1}{A} (h_\theta \bar{F}_y \theta' + h F'_y) - \mu \left(\frac{\partial \Psi'}{\partial T} + \Omega' \frac{\partial \bar{\theta}}{\partial T} + \bar{\Omega} \frac{\partial \theta'}{\partial T} \right), \quad (3.21)$$

$$\frac{\partial^2 \theta'}{\partial \tau^2} - \bar{\Omega} \Psi' - \Omega' \bar{\Psi} = -\frac{1}{A} (h_{\theta\theta} \theta' + h_\theta R' + h F'_X) - 2\mu \frac{\partial^2 \theta'}{\partial T \partial \tau}. \quad (3.22)$$

Each fluctuation is now expanded as a power series in μ :

$$f' = f'_0 + \mu f'_1 + \dots \quad (3.23)$$

Then, at leading order $O(\mu^0)$, we have the non-dissipative system

$$\frac{\partial}{\partial \tau} \left(\Omega'_0 - \Psi'_0 \cot \bar{\theta} + \frac{\bar{\Psi} \theta'_0}{\sin^2 \bar{\theta}} \right) = 0, \quad (3.24)$$

$$\frac{\partial \Psi'_0}{\partial \tau} + \bar{\Omega} \frac{\partial \theta'_0}{\partial \tau} = 0, \quad (3.25)$$

$$\frac{\partial^2 \theta'_0}{\partial \tau^2} - \bar{\Omega} \Psi'_0 - \Omega'_0 \bar{\Psi} = -\frac{1}{A} \left(h_{\theta\theta} \theta'_0 + h_\theta^2 \frac{\partial^2 \theta'_0}{\partial \tau^2} \right). \quad (3.26)$$

From (3.16c), (3.24), (3.25) and the condition that the mean of any fluctuation is zero, we find

$$\Omega'_0 = \Psi'_0 \cot \bar{\theta} - \frac{\bar{\Psi} \theta'_0}{\sin^2 \bar{\theta}} = \left(-\bar{\Omega} \cot \bar{\theta} + \frac{h_\theta}{A \bar{\Omega} \sin^2 \bar{\theta}} \right) \theta'_0, \quad (3.27)$$

$$\Psi'_0 = -\bar{\Omega} \theta'_0, \quad (3.28)$$

and substitution in (3.26) then gives

$$\frac{\partial^2 \theta'_0}{\partial \tau^2} = -\omega^2 \theta'_0, \quad (3.29)$$

where

$$\omega^2 = \frac{A}{A + h_\theta^2} \left[\bar{\Omega}^2 + \frac{1}{A} (h_{\theta\theta} + h_\theta \cot \bar{\theta}) + \left(\frac{h_\theta}{A \bar{\Omega} \sin \bar{\theta}} \right)^2 \right]. \quad (3.30)$$

Thus θ'_0 oscillates sinusoidally with frequency $\omega(T)$. Note that the relations (3.27) and (3.28), together with (3.1), imply that

$$n'_0 = 0. \quad (3.31)$$

In order to take account of dissipative effects on θ' , we need to proceed to $O(\mu)$. Equation (3.20) gives

$$\frac{\partial}{\partial \tau} \left(\Omega'_1 - \Psi'_1 \cot \bar{\theta} + \frac{\bar{\Psi} \theta'_1}{\sin^2 \bar{\theta}} \right) = -\frac{1}{A} \left(h_{\theta\theta} \hat{V}_P \theta'_0 + h_\theta^2 \hat{V}_P \frac{\partial^2 \theta'_0}{\partial \tau^2} \right), \quad (3.32)$$

from which, using (3.29),

$$\Omega'_1 = \Psi'_1 \cot \bar{\theta} - \frac{\bar{\Psi}\theta'_1}{\sin^2\bar{\theta}} + \frac{\hat{V}_P}{A} \left(\frac{1}{\omega^2} h_{\theta\theta} - h_\theta^2 \right) \frac{\partial\theta'_0}{\partial\tau}. \quad (3.33)$$

Similarly, equations (3.21) and (3.29) give

$$\frac{\partial\Psi'_1}{\partial\tau} + \bar{\Omega} \frac{\partial\theta'_1}{\partial\tau} = -\lambda \frac{\partial^2\theta'_0}{\partial\tau^2}, \quad (3.34)$$

where

$$\lambda = \frac{1}{\omega^2} \left[\frac{h_\theta}{A} \hat{V}_P + \frac{d\bar{\Omega}}{dT} + \left(\bar{\Omega} \cot \bar{\theta} + \frac{h_\theta}{A\bar{\Omega} \sin^2\bar{\theta}} \right) \frac{d\bar{\theta}}{dT} \right] - \frac{hh_\theta}{A} \hat{V}_P, \quad (3.35)$$

and it follows that

$$\Psi'_1 = -\bar{\Omega}\theta'_1 - \lambda \frac{\partial\theta'_0}{\partial\tau}. \quad (3.36)$$

Hence, the equation for θ'_1 is derived from (3.22), (3.33) and (3.36) in the form

$$\frac{\partial^2\theta'_1}{\partial\tau^2} + \omega^2\theta'_1 = -\zeta \frac{\partial\theta'_0}{\partial\tau} - 2 \frac{\partial^2\theta'_0}{\partial T \partial\tau}, \quad (3.37)$$

where

$$\zeta = \frac{1}{A + h_\theta^2} \left[\left(A\bar{\Omega} + \frac{h_\theta}{\bar{\Omega}} \cot \bar{\theta} \right) \lambda + \left\{ 2h_\theta h_{\theta\theta} - \frac{h_\theta}{h} \left(\frac{1}{\omega^2} h_{\theta\theta} - h_\theta^2 \right) \right\} \frac{d\bar{\theta}}{dT} + \frac{h^2}{|\hat{V}_P|} \right]. \quad (3.38)$$

Returning to the original time t , the equation for θ' valid up to $O(\mu)$ is now obtained by adding (3.29) and (3.37) to give

$$\ddot{\theta}' + \mu\zeta(\mu t)\dot{\theta}' + \omega^2(\mu t)\theta' + O(\mu^2) = 0. \quad (3.39)$$

(d) *Approximate solution for θ'*

Letting

$$\theta'(t) = \phi(t) \exp\left(-\frac{\mu}{2} \int_0^t \zeta(\mu t') dt'\right), \quad (3.40)$$

and neglecting terms $O(\mu^2)$, we obtain

$$\ddot{\phi} + \omega^2(\mu t)\phi = 0. \quad (3.41)$$

This may be solved approximately by the WKB method; at leading order, the solution is

$$\phi \approx c\omega^{-1/2} \cos\left(\int_0^t \omega(\mu s) ds + \xi\right), \quad (3.42)$$

where c is a constant (assumed small: $|c| \ll 1$) and ξ is the initial phase. Hence, from equation (3.40),

$$\theta' = c\Gamma \cos\left(\int_0^t \omega(\mu s) ds + \xi\right), \quad (3.43)$$

where

$$\Gamma = \omega^{-1/2} \exp(I), \quad (3.44)$$

and

$$I = -\frac{\mu}{2} \int_0^t \zeta(\mu t') dt' = -\frac{1}{2} \int_0^T \zeta(T') dT'. \quad (3.45)$$

Note that the initial perturbations θ'_0 and $\dot{\theta}'_0$ are related to c and ξ through

$$\theta'_0 = (c \cos \xi) \omega^{-1/2}|_{t=0}, \quad \dot{\theta}'_0 = c(-\omega^{1/2} \sin \xi + \dot{I} \cos \xi)|_{t=0}. \quad (3.46)$$

Under the gyroscopic condition (3.15), ω and ζ (see equation (3.38)) simplify with the aid of equation (3.16) to

$$\omega = |\bar{Q}| \left(\frac{A}{A + h_\theta^2} \right)^{1/2}, \quad (3.47)$$

and

$$\zeta = \left(-\frac{Ah_\theta}{A + h_\theta^2} \bar{Q}^2 - \frac{a^2 - 1}{A - a^2 C} \frac{AC}{A + h_\theta^2} \frac{h}{h_\theta} + \cot \bar{\theta} \right) \frac{d\bar{\theta}}{dT}. \quad (3.48)$$

In equation (3.48), the first term is dominant under the gyroscopic condition provided we are not too near either $\bar{\theta} = 0$ or $\bar{\theta} = \pi/2$ (where the second and/or third terms may become important). The integral I has the corresponding decomposition

$$I = I_1 + I_2 + I_3, \quad (3.49)$$

where

$$I_1 = \frac{A}{2} \int_{\bar{\theta}_0}^{\bar{\theta}} \frac{h_\theta \bar{Q}^2}{A + h_\theta^2} d\bar{\theta}, \quad (3.50)$$

$$I_2 = \frac{a^2 - 1}{2(A - a^2 C)} \int_{\bar{\theta}_0}^{\bar{\theta}} \frac{AC}{A + h_\theta^2} \frac{h}{h_\theta} d\bar{\theta}, \quad (3.51)$$

$$I_3 = -\frac{1}{2} \int_{\bar{\theta}_0}^{\bar{\theta}} \cot \bar{\theta} d\bar{\theta} = \frac{1}{2} \log \left(\frac{\sin \bar{\theta}_0}{\sin \bar{\theta}} \right). \quad (3.52)$$

In the following, we use the formulae (2.10) for a spheroid. The integral I_1 may be explicitly evaluated as

$$I_1 = \frac{J^2}{4A(\alpha^2 - \beta^2)} \log \left[\left(\frac{\alpha + h}{\alpha - h} \frac{\alpha - h_0}{\alpha + h_0} \right)^{1/\alpha} \left(\frac{h - \beta}{h + \beta} \frac{h_0 + \beta}{h_0 - \beta} \right)^{1/\beta} \right], \quad (3.53)$$

where $h_0 = h(\bar{\theta}_0)$, and α and β are positive constants given by

$$\alpha^2 = \frac{1}{2} \left(A + a^2 + 1 + \sqrt{(A + (a-1)^2)(A + (a+1)^2)} \right), \quad (3.54)$$

$$\beta^2 = \frac{1}{2} \left(A + a^2 + 1 - \sqrt{(A + (a-1)^2)(A + (a+1)^2)} \right). \quad (3.55)$$

Note that

$$\alpha > h > \beta, \quad \alpha > h_0 > \beta. \quad (3.56)$$

The dominant contribution to I_2 near $\bar{\theta} = 0$ or $\bar{\theta} = \pi/2$ is given by

$$I_2 \approx \frac{C}{2(a^2C - A)} \log \left[\left(\frac{\sin \bar{\theta}}{\sin \bar{\theta}_0} \right)^{a^2} \frac{\cos \bar{\theta}_0}{\cos \bar{\theta}} \right]. \quad (3.57)$$

Hence, from equations (3.44) and (3.49) to (3.57), the slowly varying amplitude Γ in equation (3.43) is given by

$$\Gamma = \omega(\bar{\theta})^{-1/2} \sigma(\bar{\theta}) \gamma(\bar{\theta})^{(1/4)J^2[A(\alpha^2 - \beta^2)]^{-1}}, \quad (3.58)$$

where

$$\gamma(\bar{\theta}) = \left(\frac{\alpha + h}{\alpha - h} \frac{\alpha - h_0}{\alpha + h_0} \right)^{1/\alpha} \left(\frac{h - \beta}{h + \beta} \frac{h_0 + \beta}{h_0 - \beta} \right)^{1/\beta} \geq 1, \quad (3.59)$$

and

$$\sigma(\bar{\theta}) = \left(\left(\frac{\sin \bar{\theta}}{\sin \bar{\theta}_0} \right)^A \left(\frac{\cos \bar{\theta}_0}{\cos \bar{\theta}} \right)^C \right)^{(1/2)(Ca^2 - A)^{-1}} \geq 0. \quad (3.60)$$

Generally, the third factor in equation (3.58) is dominant away from $\bar{\theta} = 0$ and $\bar{\theta} = \pi/2$, due to the large positive power proportional to $J^2 \sim \Omega^2$. The first factor $\omega^{-1/2}$ slightly modifies the amplitude and the second factor $\sigma(\bar{\theta})$ damps the amplitude near $\bar{\theta} = 0$ or $\pi/2$ (depending on the sign of $a^2C - A$).

Finally, we note that, using equations (3.13) and (3.39), R can be written as¹

$$R = 1 - h_\theta \omega^2 \theta' + O(\mu). \quad (3.61)$$

From this and (2.5), given that θ' is rapidly varying (so that $\dot{\theta}' = O(\mu^0)$), the dominant contribution to dR/dt is given by

$$\frac{dR}{dt} = -h_\theta \omega^2 \dot{\theta}' + O(\mu) = -W \omega^2(\bar{\theta}) + O(\mu). \quad (3.62)$$

Suppose now that, due to the growing oscillations, R first reaches zero at time $t = t_*$; then, generically, $dR/dt < 0$ and $\dot{\theta}' = O(\mu^0)$ at $t = t_*$, and it follows

¹ Here, as before, we assume that μ is small but non-zero.

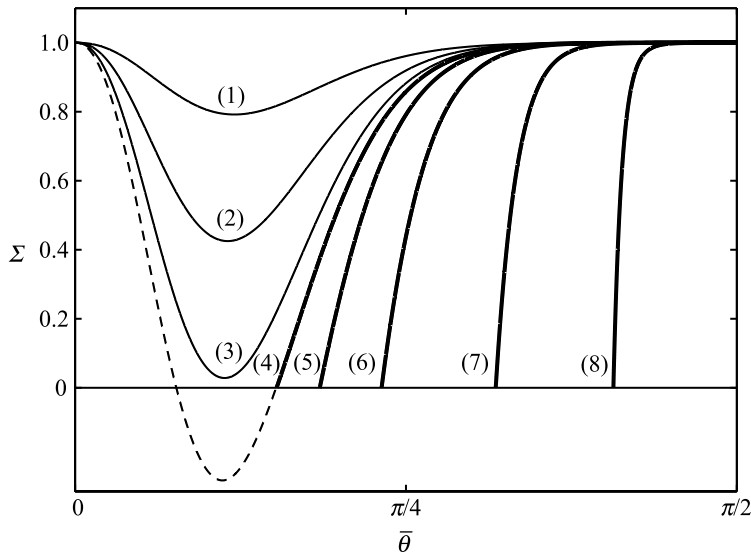


Figure 2. Slowly varying envelope Σ of the minima of the rapid oscillations in the normal reaction R as a function of $\bar{\theta}$ (equation (3.64)). A few examples are shown for a uniform prolate spheroid with $a = 1.5$, $c = -0.00054$, $\bar{\theta}_0 = \pi/2 - 0.0001$ and $J = (1) 6.20, (2) 6.50, (3) 6.63, (4) 6.70, (5) 6.83, (6) 7.15, (7) 8.45, (8) 13$. The minimum value of the envelope decreases with increasing J and finally becomes negative which indicates jumping. The spheroid then enters a different dynamical regime and the remaining part of the contour (shown as a dashed curve) becomes inapplicable. For the larger values of J (thick curves) the inclination angle at which the jump takes place approaches the initial angle $\bar{\theta} \approx \pi/2$.

from equation (3.62) that

$$W = W_* > 0, \quad \text{at } t = t_*, \quad (3.63)$$

that is, the centre-of-mass is rising at the moment when R first reaches zero.

Using equations (3.43) and (3.61), the slowly varying envelope of the minima of the rapid oscillations in R can be approximated (including only $O(\mu^0)$ terms) by

$$\Sigma \approx 1 - |h_\theta \omega^2 c \Gamma|. \quad (3.64)$$

A few contours of this envelope are presented in [figure 2](#) for a uniform prolate spheroid with $a = 1.5$ and a range of values of the Jellett constant J . In each case, a perturbation corresponding to $c = -0.00054$ is introduced at $\bar{\theta}_0 = \pi/2 - 0.0001$. For increasing values of J , the minimum of the envelope approaches zero and eventually becomes negative. However, R cannot become negative and the moment $t = t_*$ of violation of the constraint $R \geq 0$ indicates loss of contact between the spheroid and the table. In this situation, the remaining part of the envelope (a dashed curve) is inapplicable, since the spheroid enters a different dynamical regime of ‘free motion’ under the action of gravity alone. If J is increased further (thick curves), the inclination angle at which the spheroid first loses contact with the table approaches the initial angle $\bar{\theta}_0$ (the same holds for oblate spheroids). The validity of the formula (3.64) is supported by the numerical simulations to be presented in §§5 and 6 below.

4. Self-induced jumping

In this section, we consider the situation when R does fall to zero as a result of growing oscillations, as described above. Let us shift the origin of time to the instant $t = t_*$ when this occurs (i.e. replace $t - t_*$ by t). Since R cannot become negative, it must remain zero for some finite interval of time $t > 0$, during which the spheroid is in ‘free’ motion, for which the centre-of-mass is subject to gravitational acceleration $-\mathbf{K}$, and the rotation relative to O is governed by Euler’s equations. Note that dR/dt is discontinuous at $t = 0$. As we pass from constrained motion for $t < 0$ to free motion for $t > 0$, the body experiences no impulse and the forces acting on the body are continuous through $t = 0$. It follows that the velocity and acceleration of any point of the body are continuous through $t = 0$. However, since dR/dt is discontinuous, the time-derivative of the accelerations are correspondingly discontinuous at $t = 0$. We shall use the suffix $*$ to denote conditions at $t = 0+$.

Let P continue to denote the lowest point of the spheroid even when it loses contact with the table, and let $\Delta(t)$ represent the gap between the spheroid and the table, i.e. the height of P above the table, for $t > 0$. We continue to denote the vertical projection of OP by $h(\theta)$ as given by equation (2.10). Then Δ is given by

$$\Delta = h_* + W_* t - \frac{1}{2} t^2 - h(\theta), \quad (4.1)$$

for $t > 0$ during the free motion. From equations (2.5) and (2.8), with $R = 0$ at $t = 0$, we find

$$\dot{h}|_{t=0} = \dot{h}_* = W_*, \quad \ddot{h}|_{t=0} = \ddot{h}_* = -1, \quad (4.2)$$

and, for the reasons given above, these quantities are continuous through $t = 0$. Hence the Taylor expansion of h for small $t > 0$ gives

$$\Delta = -\frac{1}{6} h_*^{(3)} t^3 - \frac{1}{24} h_*^{(4)} t^4 + \dots, \quad (4.3)$$

where $h_*^{(3)} = d^3 h/dt^3|_{t=0+}$, $h_*^{(4)} = d^4 h/dt^4|_{t=0+}$. This description is self-consistent only if $h_*^{(3)} < 0$ (as will be established—see equation (4.20) below), and then equation (4.3) shows that the initial growth of Δ during the stage of free motion is cubic in t . Note that the third and higher time derivatives of h are discontinuous at $t = 0$ and must here be evaluated at $t = 0+$.

For the evaluation of h when $t > 0$, we need to know the time evolution of θ for $t > 0$; this is described by the system of equations (3.3) with $R = 0$:

$$\frac{d}{dt}(\Omega - \Psi \cot \theta) = 0, \quad (4.4a)$$

$$\frac{d\Psi}{dt} + \Omega \frac{d\theta}{dt} = 0, \quad (4.4b)$$

$$\frac{d^2\theta}{dt^2} - \Omega\Psi = 0. \quad (4.4c)$$

The variables Ω , Ψ , θ and $\dot{\theta}$ are all continuous through $t = 0$, so we may adopt initial conditions

$$\Omega(0) = \Omega_*, \quad \Psi(0) = \Psi_*, \quad \theta(0) = \theta_*, \quad \dot{\theta}(0) = \dot{\theta}_*, \quad (4.5)$$

where these quantities are determined by the foregoing analysis up to the instant $t=0$ when the condition $R=0$ is first satisfied. The system (4.4) is well known in analytical dynamics (e.g. Marsden & Ratiu 1999) and can be integrated explicitly. Note first the three constants of motion,

$$\Omega - \Psi \cot \theta = C_1, \quad (4.6)$$

$$\Psi^2 + \dot{\theta}^2 = C_2^2, \quad (4.7)$$

and

$$\Omega \cos \theta - \frac{\Psi}{\sin \theta} = n_0. \quad (4.8)$$

Now from equation (4.4*b*), we have

$$\frac{d\Psi}{d\theta} = -\Omega = -(C_1 + \Psi \cot \theta), \quad (4.9)$$

so that

$$\Psi = C_1 \cot \theta + C_1' \operatorname{cosec} \theta, \quad (4.10)$$

where

$$C_1' = \Psi_* \operatorname{cosec} \theta_* - \Omega_* \cos \theta_*. \quad (4.11)$$

Using equations (4.7) and (4.10), the solution for θ is then found in the form

$$\cos \theta = -C_4 - C_3^{-1} \dot{\theta}_* \sin \theta_* \sin C_3 t + (\cos \theta_* + C_4) \cos C_3 t, \quad (4.12)$$

where

$$C_3^2 = C_1^2 + C_2^2 = (\Omega_* - \Psi_* \cot \theta_*)^2 + \Psi_*^2 + \dot{\theta}_*^2, \quad (4.13)$$

$$C_4 = C_1 C_1' C_3^{-2} = (\Omega_* - \Psi_* \cot \theta_*)(\Psi_* \operatorname{cosec} \theta_* - \Omega_* \cos \theta_*) C_3^{-2}. \quad (4.14)$$

Hence, $h(\theta)$ and so $\Delta(t)$ are obtained explicitly from equations (2.10) and (4.1).

The solution (4.12) may be simplified if we assume the gyroscopic condition (3.15). Note first that, if we set $R=0$ in equation (3.61), then θ'_* can be expressed (up to $O(\mu)$ and with $\Omega_* \approx \bar{\Omega}_*$) as

$$\theta'_* = \frac{1}{h_{\theta_*} \omega_*^2} \approx \frac{A + h_{\theta_*}^2}{A h_{\theta_*} \Omega_*^2}, \quad (4.15)$$

and also that, using (3.16*c*), (3.28) and (4.15), Ψ_* can be expressed as

$$\Psi_* = \bar{\Psi}_* + \Psi_*' \approx h_{\theta_*} (A \Omega_*)^{-1} - \Omega_* \theta'_* \approx (\Omega_* h_{\theta_*})^{-1}. \quad (4.16)$$

Hence, since θ' oscillates with frequency $O(\Omega_*)$, under this gyroscopic approximation both θ_* and Ψ_* are $O(\Omega_*^{-1})$, and so

$$\left. \begin{aligned} C_3^2 &= \Omega_*^2 + 2h_{\theta_*}^{-1} \cot \theta_* + O(\Omega_*^{-2}), \\ C_4 &= -\cos \theta_* - (\Omega_*^2 h_{\theta_*})^{-1} \sin \theta_* + O(\Omega_*^{-4}). \end{aligned} \right\} \quad (4.17)$$

During the initial stage of evolution (when $|\theta - \theta_*|$ is small), the solution (4.12) thus simplifies to

$$\theta = \theta_* + \frac{\cos \Omega_* t - 1}{h_{\theta_*} \Omega_*^2} + \frac{\dot{\theta}_* \sin \Omega_* t}{\Omega_*}. \quad (4.18)$$

Using (4.18), we now obtain

$$\left. \frac{d^3 \theta}{dt^3} \right|_{t=0+} = -\Omega_*^2 \dot{\theta}_*, \quad \left. \frac{d^4 \theta}{dt^4} \right|_{t=0+} = \frac{\Omega_*^2}{h_{\theta_*}}, \quad (4.19)$$

and hence, at leading order in Ω_* ,

$$h_*^{(3)} \approx h_\theta \left. \frac{d^3 \theta}{dt^3} \right|_{t=0+} = -h_{\theta_*} \Omega_*^2 \dot{\theta}_* = -W_* \Omega_*^2, \quad (4.20)$$

$$h_*^{(4)} \approx h_\theta \left. \frac{d^4 \theta}{dt^4} \right|_{t=0+} = \Omega_*^2. \quad (4.21)$$

Here we note that, since W_* is positive, $h_*^{(3)}$ is indeed negative, as required for self-consistency.

Finally, combining equations (4.3), (4.20) and (4.21), the gap Δ is given to $O(t^4)$ by

$$\Delta = \frac{1}{24} \Omega_*^2 t^3 (4W_* - t) + \dots \quad (4.22)$$

This provides a good approximation for $t \ll 1$. Provided $W_* \ll 1$, equation (4.22) indicates that the spheroid returns to the table at $t = 4W_*$, which is within the range of validity of this approximation. The gap attains a maximum value

$$\Delta_{\max} = \frac{9}{8} \Omega_*^2 W_*^4 \quad (4.23)$$

when $t = 3W_*$. Now $W_*(=h_{\theta_*} \dot{\theta}_*)$ is, as already indicated, determined by the earlier constrained motion and depends on the amplitude and phase of the oscillatory modes that may be present (c and ξ in equation (3.43)). The best that we might hope (in circumstances when the condition $R = 0$ is attained) would be to obtain a useful upper bound for W_* in terms of μ and the initial angular velocity of the spheroid. The computations presented below suggest that Δ_{\max} is (as might be expected) very small (of order 10^{-2} at most in the results shown—see figure 5) and that Δ_{\max} decreases rapidly with increasing Ω_0 (asymptotically like Ω_0^{-5}).

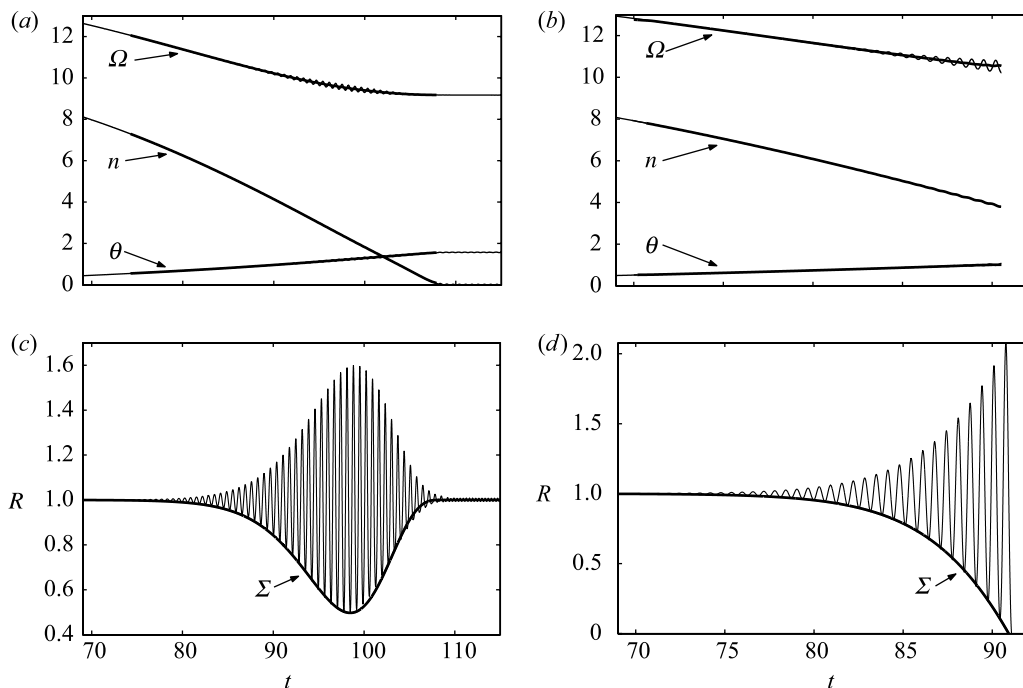


Figure 3. Time evolution (for $t > 70$) of Ω , θ , n and the normal reaction R for an oblate spheroid with $a=2/3$ (Coulomb friction with $\mu=0.1$). The thin lines show the numerical simulation; the thick lines represent the gyroscopic solutions (a,b), and the analytical estimate Σ of the slowly varying envelope of the minima (3.64) (c,d). The initial perturbation corresponds to $c = 0.00052$ in both cases (see equations (3.43) and (3.64)). (a,c) $n_0=10$; $J=4$; spheroid rises all the way without jumping and the oscillations of R are eventually damped. (b,d) $n_0=10.5$; $J=4.2$; oscillations amplify until R vanishes at $t = t_* \approx 91$ when the spheroid loses contact with the table during its rise.

5. Numerical treatment

We now present the results of computations based on the exact system (2.7). Here, as in part I, we used an implicit time-adaptive method based on second-order numerical differentiation formulae, similar to that described by [Shampine \(1980\)](#). We imposed a relative error tolerance 10^{-9} in the runs presented here.

In §3, we obtained an analytical estimate for the slowly varying envelope Σ of the rapid oscillations in the normal reaction R (see equation (3.64)). Here, we test this estimate against direct numerical simulations performed first for a uniform oblate spheroid with $a=2/3$ and second for a uniform prolate spheroid with $a=3/2$. Coulomb friction with $\mu=0.1$ was used.

Figure 3 shows the computed evolution of Ω , θ , n and R for a uniform oblate spheroid during its rise from the state of steady spin with axis of symmetry vertical towards the state of steady precession with axis of symmetry precessing in a horizontal plane. Two distinct scenarios are shown, corresponding to evolution from two different unstable steady spin states with $n_0=10$ and 10.5. In both cases the perturbation is applied along the vector in phase space with

components (approximately)

$$U = 8 \times 10^{-7}, \quad V = 4 \times 10^{-6}, \quad \Omega = C n_0 A^{-1}, \quad A = 10^{-5}, \quad \theta = 4 \times 10^{-6}, \quad n_0. \quad (5.1)$$

For $n_0 = 10$ (figure 3*a,c*), the spheroid rises all the way to the state of steady horizontal precession without jumping and the initially growing oscillations evident in R are eventually damped. For a slightly larger initial spin, $n_0 = 10.5$, these oscillations amplify until the spheroid loses contact with the table. In both cases, the gyroscopic solutions (thick lines in figure 4*a,c*) approximate the exact dynamics very well in the mean, in the latter case until the moment of jumping. Moreover, the analytical formula (3.64) (thick lines in figure 3*b,d*) represents quite accurately the envelope of the rapid oscillations.

The results of corresponding computations for the prolate case are presented in figure 4, where the normal reaction (thin line) is plotted as the spheroid rises from an unstable state of steady precession with its axis of symmetry horizontal towards the state of steady spin with the axis of symmetry vertical. Two scenarios are shown corresponding to evolution with two different initial precession rates, $\Omega_0 = 10.2$ and 10.5. In both cases, the horizontal precession state is perturbed in the unstable direction with initial conditions (approximately)

$$U = 7 \times 10^{-5}, \quad V = 2 \times 10^{-6}, \quad \Omega_0, \quad A = -10^{-4}, \quad \theta = \frac{\pi}{2} - 10^{-3}, \quad n = 2 \times 10^{-2}. \quad (5.2)$$

In figure 4*a* ($\Omega_0 = 10.2$), the spheroid rises all the way to the vertical without jumping and the initially growing oscillations are eventually damped. In figure 4*b* ($\Omega_0 = 10.5$), the oscillations amplify until R hits zero and the spheroid loses contact with the table. In both cases, the analytical formula (3.64)—represented by the thick lines—provides an excellent approximation for the slowly varying envelope of the minima of the rapid oscillations.

Finally, figure 5*a–c* shows the time variation of the gap Δ given by equation (4.1) for various values of Ω_0 . The solid lines are the result of the full numerical simulation, while the broken line shows the analytical result (4.22) using the computed data for Ω_* and W_* . The differences result from the approximations used in deriving equations (4.20) and (4.21); as expected, these differences decrease with increasing Ω_0 . Figure 5*d* shows the maximum of the gap Δ_{\max} as given by equation (4.23) (see caption for details); the points are bounded above by the curve $\Delta_{\max} = (4.65/\Omega_0)^5$ shown in the figure.

6. Determination of the ‘jump’ surface

We aim here to determine the geometry of the boundary $R = 0$ which marks the transition between the constrained and the free dynamics. In general, this boundary is a five-dimensional ‘surface’ in the six-dimensional phase space $\mathcal{E} = (U, V, \Omega, A, \theta, n)$, and cannot be usefully projected onto the three-dimensional subspace (Ω, θ, n) used previously in part I. However, if we focus on dynamics in the neighbourhood of the unstable manifold in the ‘gyroscopic’ region of the phase space, a useful approximation can be derived.

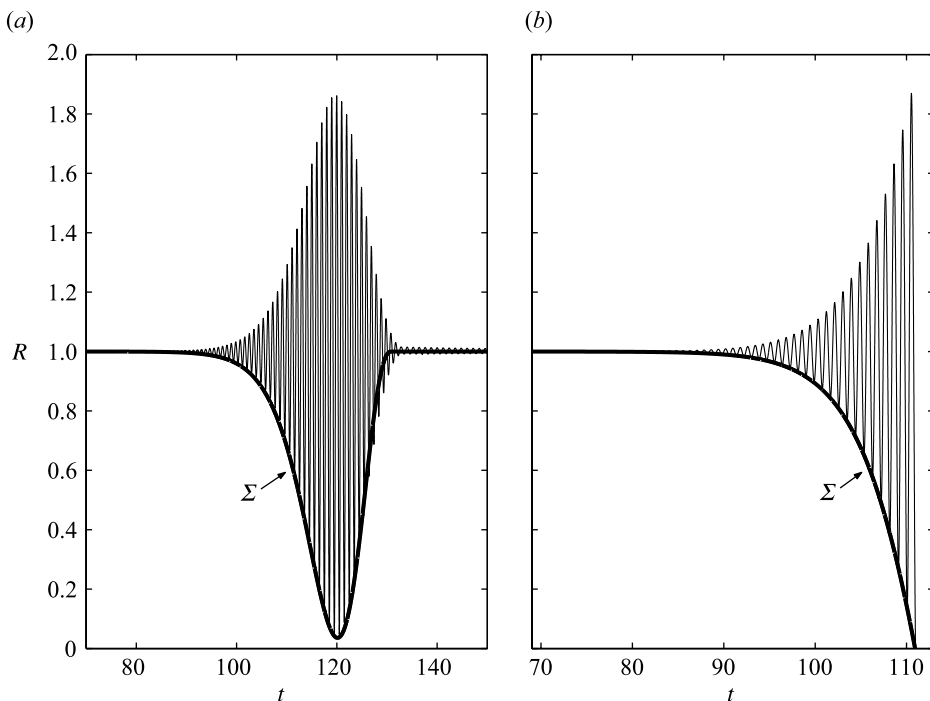


Figure 4. Same as figure 3*c,d*, but for a prolate spheroid with $a = 3/2$ and $c = -0.00054$. (a) $\Omega_0 = 10.2$; $J = 6.63$; spheroid rises all the way without jumping and the oscillations of R are eventually damped. (b) $\Omega_0 = 10.5$; $J = 6.83$; oscillations amplify until R vanishes at $t = t_* \approx 111$, when the spheroid loses contact with the table.

Let us first rewrite the normal reaction (2.8), as given by equation (3.14) in part I, in the form

$$R = \frac{A + Ah_{\theta\theta}A^2 + \Omega h_{\theta} \sin \theta (A\Omega \cos \theta - Cn)}{A + h_{\theta}(h_{\theta} - \mu h \hat{U}_P)}, \quad (6.1)$$

where $\hat{U}_P = U_P/|U_P|$. As shown in part I and the previous sections, $A (= \dot{\theta} + \dot{\theta}')$ remains $O(\max(\mu, \dot{\theta}'))$ in the neighbourhood of the unstable manifold during the process of rising. Hence, in the gyroscopic region of the phase space where $\Omega^2/|a^2 - 1| \gg 1$, and away from the immediate vicinity of $\theta = 0$ and $\theta = \pi/2$, the second term in the numerator of equation (6.1) may be omitted in first approximation. Thus,

$$R \approx \frac{A + \Omega h_{\theta} \sin \theta (A\Omega \cos \theta - Cn)}{A + h_{\theta}^2}, \quad (6.2)$$

and the boundary $R = 0$ is then given by

$$n = \frac{A}{C} \left(\Omega \cos \theta + \frac{1}{\Omega h_{\theta} \sin \theta} \right), \quad (6.3)$$

a two-dimensional surface imbedded in the subspace of the variables (Ω, θ, n) . If we now use the transformation (3.1) and adopt the multiple-scale terminology

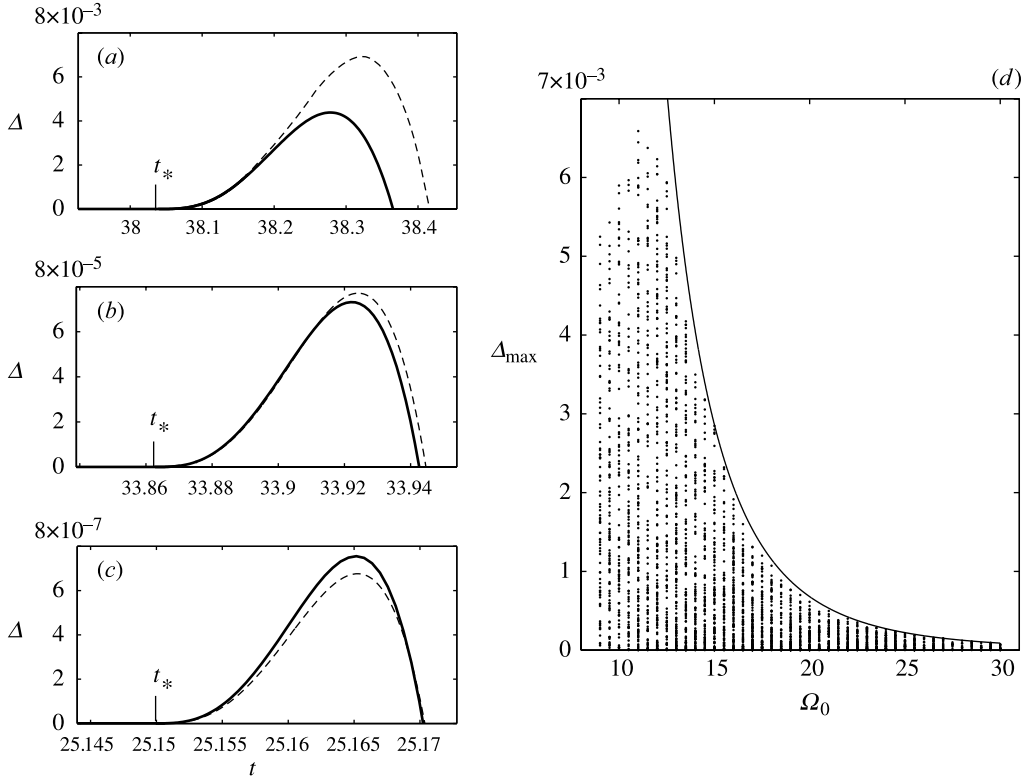


Figure 5. The gap Δ (4.1) versus time t , for $\Omega_0 =$ (a) 11, (b) 20, (c) 30. The solid line in each case shows the full numerical simulation, and the broken line plots (4.22) with the computed data for Ω_* and W_* . (d) Maximum of the gap, Δ_{\max} , for a range of values of Ω_0 ; the points on each vertical line correspond to different initial perturbations of amplitude 0.05 and random direction. The upper bounding curve is $\Delta_{\max} = (4.65/\Omega_0)^5$.

used in previous sections, R can be further approximated (using also equations (3.16c), (3.28) and (3.47)) by

$$R \approx \frac{A + Ah_\theta(\bar{Q}\bar{\Psi} + \bar{Q}\Psi')}{A + h_\theta^2} \approx 1 - \frac{A\bar{Q}^2 h_\theta \theta'}{A + h_\theta^2} + O(\mu) = 1 - h_\theta \omega^2 \theta' + O(\mu). \quad (6.4)$$

Thus, the approximation (6.2) is consistent with the multiple-scale result (3.61).

An example of the ‘jump’ surface (6.3) is shown in figure 6a for a uniform prolate spheroid with $a = 1.5$. The trajectories shown represent evolution towards the stable equilibrium with $\theta = 0$ from the neighbourhood of the unstable horizontal precession with $\theta = \pi/2$; Coulomb friction with $\mu = 0.1$ was used. The initial perturbation was applied in the unstable direction with amplitude $\delta = 0.01$ for a number of different initial precession values Ω_0 . As shown in part I, the unstable direction in the linearization around the fixed point ($U = 0, V = 0, \Omega_0, A = 0, \theta = \pi/2, n = 0$) corresponds to a non-oscillatory mode. In the simulation, the exact expression for the normal reaction (6.1) was monitored, and the calculation was terminated when the trajectory crossed the boundary, i.e. when $R = 0$ and $dR/dt < 0$. The surface shown is the

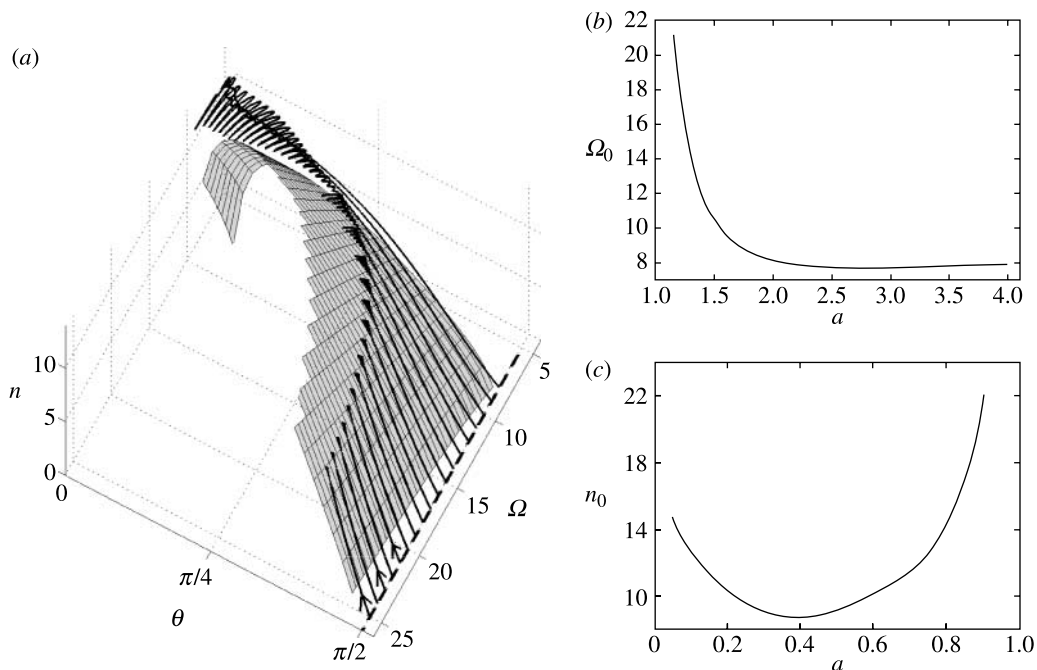


Figure 6. (a) The jump surface (6.3) and a set of trajectories which evolve towards the stable equilibrium at $\theta = 0$ and which terminate when $R = 0$ (uniform prolate spheroid with $a = 1.5$, Coulomb friction with $\mu = 0.1$; perturbation applied in the unstable non-oscillatory direction at $\theta = \pi/2$). (b) Relation (derived numerically) between the aspect ratio ($a > 1$) of a prolate spheroid and the smallest initial rate of precession Ω_0 which leads to eventual loss of contact with the table. (c) Same as (b), but for an oblate spheroid ($a < 1$) and with n_0 the smallest initial spin that leads to a jump.

approximated jump surface (6.3). It is clear that this approximated jump surface detects the moment of jumping very well. More importantly, however, we note that the distance between the unstable manifold and the jump surface $R = 0$ is small and decreases with Ω : the unstable manifold appears to ‘shadow’ the jump surface. Trajectories which originate from arbitrary perturbations (not exactly along the unstable manifold), and which therefore tend to oscillate vigorously from the start, consequently cross the boundary at a much earlier stage of evolution. This is probably the situation in most real-life experiments. Note also that with increasing Ω_0 , the angle θ at which the respective trajectory crosses the jump surface approaches the initial angle θ_0 ($\approx \pi/2$ for the case of the prolate spheroid). This is again in qualitative agreement with the analytical predictions summarized in figure 2.

Figure 6b presents the numerically determined relation between the parameter a and the smallest initial value of the rate of precession Ω_0 for which the trajectory, evolving along the unstable manifold, eventually crosses the boundary $R = 0$. The initial perturbation is applied in the unstable direction at the appropriate fixed point with amplitude $\delta = 0.01$. Figure 6c presents corresponding results for the oblate spheroid and shows the relation between a and the smallest initial value of spin n_0 that leads to a jump. It should be stressed that for a general perturbation, which includes an admixture of oscillatory modes, the

overall contour would shift downwards; this is again due to the fact that the unstable manifold ‘shadows’ the jump surface. The rise of the curves of figure 6*b,c* as $a \rightarrow 1$ allow us to conclude, however, that for given perturbation, spheroids with $|a - 1| \ll 1$ do not easily lose contact with the surface, and an increasingly large initial angular velocity is required to induce a jump as $a \rightarrow 1$. This is because it is the product Ωh_θ that appears in the expression (6.2) for R , and $h_\theta \rightarrow 0$ as $a \rightarrow 1$.

7. Conclusions

The following results have been found analytically and confirmed numerically. There are situations when the normal reaction R for a spinning spheroid oscillates with an initially growing amplitude. When the initial angular momentum is sufficiently large, oscillatory modes can grow to such an extent that R falls to zero. This implies loss of contact between the spheroid and the table (i.e. self-induced jumping), and the spheroid passes temporarily into a state of free motion under gravity without friction. The exact solution for this free motion shows that the gap between the spinning spheroid and the table increases as t^3 in the initial stage of jumping. The short duration of free motion before contact is re-established is determined approximately.

Thus, a spheroid which is spun sufficiently rapidly on a table will, in general, lose contact with the table at some stage during its rising motion. We have considered the free motion only until the first bounce; however, the subsequent behaviour presumably consists of rapidly alternating periods of motion with and without frictional contact with the table. The details of the successive impacts depend on the elastic/plastic properties of both the spheroid and the table. This is clearly a subject for future investigation, both experimental and computational. Irrespective of the details, however, as stated in §1, we may conjecture that the averaged effect (over many successive impacts) will be simply to give an ‘effective’ Coulomb friction parameter μ_e somewhat less than the instantaneous value of μ that holds during the periods of continuous contact.

Y.S. would like to dedicate this paper to Professor Akira Yoshizawa on his retirement from the University of Tokyo. He thanks the Daiwa Anglo-Japanese Foundation, Trinity College, Cambridge and Keio University for their financial support. M.B. is supported by a scholarship of the Gates Cambridge Trust. H.K.M. acknowledges the support of the Fondation de l’Ecole Normale Supérieure, Paris, through his tenure of the Chaire Internationale de Recherche Blaise Pascal (2001–2003) when this work was initiated, and also the support of a Leverhulme Emeritus Professorship (2004–2005).

References

- Bloch, A. M., Krishnaprasad, P. S., Marsden, J. E. & Ratiu, T. S. 1994 Dissipation induced instabilities. *Ann. Inst. H. Poincaré, Analyse Nonlinéaire* **11**, 37–90.
- Bou-Rabee, N. M., Marsden, J. E. & Romero, L. A. 2004 Tippe top inversion as a dissipation-induced instability. *SIAM J. Appl. Dyn. Syst.* **3**, 352–377.
- Bou-Rabee, N. M., Marsden, J. E. & Romero, L. A. 2005 A geometric treatment of Jellett’s egg. *Z. Angew. Math. Mech.* **85**(8), 1–25.
- Hinch, E. J. 1992 *Perturbation methods*. Cambridge: Cambridge University Press.
- Holmes, M. H. 1995 *Introduction to perturbation methods*. New York: Springer.
- Proc. R. Soc. A* (2005)

- Marsden, J. & Ratiu, T. S. 1999 *Introduction to mechanics and symmetry*. New York: Springer.
- Moffatt, H. K. & Shimomura, Y. 2002 Spinning eggs—a paradox resolved. *Nature* **417**, 385–386.
- Moffatt, H. K., Shimomura, Y. & Branicki, M. 2004 Dynamics of an axisymmetric body spinning on a horizontal surface. I. Stability and the gyroscopic approximation. *Proc. R. Soc. A.* **460**, 3643–3672.
- Shampine, L. F. 1980 Implementation of implicit formulas for the solution of ODE's. *SIAM J. Sci. Stat. Comput.* **1**, 103–118.
- Yoshizawa, A. 1984 Statistical analysis of the deviation of the Reynolds stress from its eddy-viscosity representation. *Phys. Fluids* **27**, 1377–1387.
- Yoshizawa, A. 1998 *Hydrodynamic and magnetohydrodynamic turbulent flows: modeling and statistical theory*. Dordrecht: Kluwer Academic.